LRP 531/95 October 1995

Invited and Contributed Papers
presented at the
20TH INTERNATIONAL CONFERENCE
ON INFRARED AND MILLIMETER WAVES

Lake Buena Vista, Orlando, USA
December 11 - 14, 1995

Content

Particle-In-Cell (PIC) Simulations of Beam Instabilities in Gyrotron Beam Tunnels

T.M. Tran, G. Jost, K. Appert, O. Sauter and S. Wuthrich*

CRPP, Association Euratom-Confédération Suisse,
Ecole Polytechnique Fédérale de Lausanne, CH-1007 Lausanne, Switzerland

* CRAY Research, PATP/PSE, EPFL, CH-1015 Lausanne, Switzerland

Abstract

Experimental observations seem to indicate that the beam velocity and energy spreads are larger than those calculated from the electron trajectory codes which do not take into account the effects of beam instabilities. On the other hand, parasitic oscillations of the beam with frequencies close to the electron cyclotron frequency ω_{ce} have been observed experimentally, suggesting the possibility that instabilities can be excited in the beam tunnels and are responsible for the beam degradation. 2D electrostatic and electromagnetic time-dependent PIC codes have been developed to simulate the beam transport in the beam tunnel. The results of extensive parametric runs, using these codes (which were ported on the Cray T3D massively parallel computer), together with the role of the beam instabilities around ω_{ce} on the beam degradation will be reported.

Introduction

Linear and nonlinear analyses of the electrostatic electron cyclotron instability in electron beams [1–3] suggest that this type of instability might be responsible for the degradation of the beam quality observed in gyrotrons. In this paper, electrostatic and electromagnetic PIC codes are presented and used to investigate this beam degradation problem.

Simulation models

Two PIC simulation codes have been developed to study the beam instabilities in gyrotron beam tunnels: the G2D code based on the electrostatic (ES) approximation and the G2DTM code modeling the transverse magnetic (TM) components of the electromagnetic fields. In both codes cylindrical symmetry is assumed and the particles are fully relativistic; the five-dimensional phase space is described by $(r, z, p_r, p_\theta, p_z)$, where $\vec{p}$ denotes the momentum. The main characteristics of each code can be summarized as follows.

G2D code

1. Linear charge assignment [4–5].
2. Bilinear approximation for the electric potential ϕ: the component of the electric field E_r is then piecewise *linear* in z and piecewise *constant* in r while the component of the electric field E_z is piecewise *linear* in r and piecewise *constant* in z.
3. Poisson solver using a domain decomposition technique that allows to consider complex geometries (as in beam tunnels with an opening, as found in quasi-optical gyrotrons).

G2DTM code

1. Piecewise linear-constant approximation for E_r, E_z as in G2D and piecewise constant approximation for B_θ.
2. Eastwood's current assignment [6] which enforces the charge conservation.
3. Absorbing boundary layers at both ends of the beam tunnel using the scheme of Ref. [7] to model the open boundary conditions for the electromagnetic field.

In both codes the beam is injected at the left end of the beam tunnel, using a Gaussian distribution in p_z and $p_\perp = \sqrt{p_r^2 + p_\theta^2}$, and a uniform distribution for the gyro-angles. A profile in the guiding-center radius can also be specified. The right end is modeled as a perfectly absorbing wall for the particles.

In order to perform long runs, both codes are parallelized and most of the production runs are performed on the Cray-T3D using up to 256 processors.

Simulation results

a) Electrostatic simulations with G2D

We considered a cylindrical beam tunnel of length $L = 20\,\text{cm}$, radius $R_w = 5\,\text{mm}$ and with an opening at its center of 7.5 cm. A thin annular electron beam (radius $R_g = 3\,\text{mm}$) is injected at the left end with $V_0 = 80\,\text{kV}$ and $\alpha = p_\perp/p_z = 1.5$. The guiding magnetic field is assumed uniform with $B_0 = 4\,\text{T}$. The geometry considered represents in fact a section of a whole magnetron injection gun which has been simulated by the *time-independent* code Daphne [8]

The transverse velocity spreads, obtained by such a code and thus induced by only the beam optics (at the cathode) are displayed in Fig. 1 as disconnected points. The results calculated from the electrostatic G2D code are shown by the two continuous curves for the injection of a cold and a hot beam, respectively. In the hot beam case, the initial spreads are taken equal to those calculated by Daphne.

As shown in Fig. 1, in the cold beam case, the electrostatic instability can occur even at small beam currents, inducing thus a velocity spread which increases with the current. However, when the beam optics induced spreads are taken into account (hot beam case), a degradation of the beam quality occurs only at high values of the beam current.

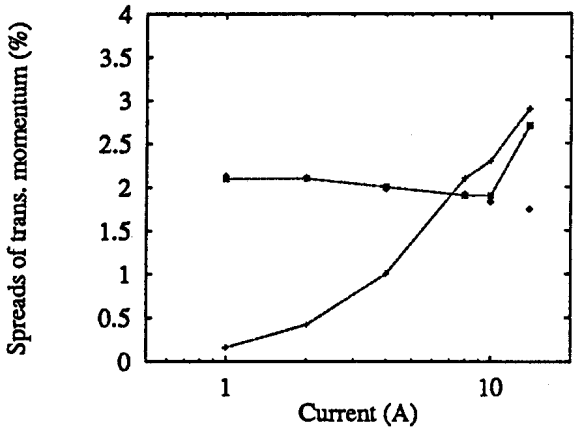

Figure 1: The spreads obtained for a cold beam (+) and a hot beam (∗). The spreads calculated from the Daphne code are displayed as disconnected symbols (◇).

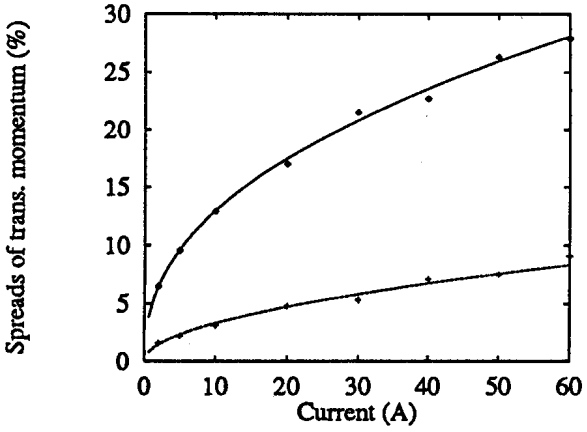

Figure 2: The spreads obtained from G2DTM (upper curve) and from G2DP (lower curve)

Experimental measurements of the velocity spread [9] indicate on the other hand that the beam is already degraded at currents as low as 1 A.
Quantitatively similar results have been found for a beam tunnel without opening, implying that the strong beam electrostatic depression across the opening has no effect on the electrostatic instability.
Finally, we have simulated the imperfect vacuum in the beam tunnel by introducing a cold neutral background plasma in G2D. Beam-plasma instabilities with a strong effect on the beam can indeed be excited when the background plasma is dense enough. In the considered cylindrically symmetric case, the density must, however, be unrealistically high (at least as high as the beam electron density !).

b) Electromagnetic simulations with G2DTM
In the following runs, a straight cylindrical beam tunnel with $L = 10\,\text{cm}$ and $R_w = 5\,\text{mm}$ is considered. The injected beam is cold and has the following parameters: $\alpha = 1.5$, $V_0 = 80\,\text{kV}$, $B_0 = 3.8\,\text{T}$ and $R_g = 3\,\text{mm}$. The maximum transverse velocity spread, calculated by G2D and G2DTM are both shown versus the beam current in Fig. 2. In the G2DTM runs, we have observed the excitation of a backward wave. The measured frequency and wavelength satisfy the Doppler down-shifted dispersion relation $\omega = \omega_{ce} - k_z v_z$ and correspond to a TM_{03} cavity mode. This is confirmed by the field radial profile. This backward wave, which can interact strongly with the beam, is thus responsible for the observed large transverse velocity spread. Because the wave couples with the particles mainly through its transverse component E_r, no additional increase of the *axial* velocity spread has been observed in the electromagnetic simulations, in contrast to the experimental findings [9].

Conclusion

Extensive runs using the electrostatic PIC code G2D show that the cylindrically symmetric electrostatic electron cyclotron instability cannot explain the large velocity spreads observed experimentally in cylindrical as well as as in quasi-optical gyrotrons. The main reason is that the electron beam density in these devices are usually small. On the other hand, electromagnetic simulations subject to the same symmetry constraint seem to indicate that cavity modes can be excited in the beam tunnel and enhance the perpendicular velocity spread through a backward wave interaction with the beam.

Acknowledgments

This work was supported in part by the Swiss National Science Foundation and by Cray Research, Inc. within the framework of the Cray Research/EPFL Parallel Application Technology Program. The computations were done on the Cray T3D massively parallel computer at EPFL, Lausanne.

References

[1] F.S.Kuo, K.R. Chu, Chinese J. Phys. 28 (1990) 327.
[2] A. Bondeson, T.M. Antonsen, Int. J. Electron. 61 (1986) 855.
[3] V.L. Bratman, A.V. Savilov, Phys. Plasmas 2 (1995) 557.
[4] C.K. Birdsall, A.B. Langdon, *Plasma Physics via Computer Simulation*, McGraw-Hill Inc., 1985.
[5] R.W. Hockney, J.W. Eastwood, *Computer Simulation using Particles*, Adam Hilger Inc., 1988.
[6] J.W. Eastwood, Comput. Phys. Commun. 64 (1991) 252.
[7] J.P. Berenger, J. Comput. Phys. 114 (1994) 185.
[8] T.M. Tran, D.R. Whaley, S. Merazzi, R. Gruber, Proc. 6th joint EPS-APS Int. Conf. on Physics Comput. PC94, 491 (1994).
[9] G. Soumagne, *Mesure de la fonction de distribution de vitesse du faisceau d'électrons d'un gyrotron quasi-optique*, thèse N°1390 (1995), Ecole Polytechnique Fédérale de Lausanne.

Electron Cyclotron Emission as e-beam Diagnostic: Interpretation of Experimental Results

S. Alberti, M. Pedrozzi, M.R. Siegrist, G. Soumagne, M.Q. Tran, T.M. Tran

Centre de Recherches en Physique des Plasmas,
Association Euratom - Confédération Suisse,
Ecole Polytechnique Fédérale de Lausanne,
21, Avenue des Bains, 1007 Lausanne, Switzerland

Abstract

We present time-resolved measurements and an analysis of the parallel velocity distribution function of the e-beam in a quasi-optical gyrotron based on electron cyclotron emission. Since such measurements are performed at full beam parameters, perturbative effects, e.g. parasitic oscillations in the beam tunnel, are also observed contrary to standard diagnostics using scaled e-beam parameters. Considerations on ECE-measurements of the e-beam energy spread, which may be caused by parasitic oscillations, are also discussed.

Introduction

Electron Cyclotron Emission (ECE) has been proven to be an efficient non-intrusive diagnostic for in situ characterization of gyrotron e-beams [1]. The Doppler shifted frequency, ω, emitted by a test electron in the direction θ with respect to the applied magnetic DC-field is given by:

$$\omega = \frac{\Omega_o}{\gamma(1 - \beta_\parallel \cos\theta)}$$

where Ω_o is the non-relativistic cyclotron frequency, γ is the relativistic factor and $\beta_\parallel$ the normalized parallel velocity. This relation indicates that the observed frequency depends simultaneously on the test electron energy and its parallel velocity. The measurement of the ECE-spectrum of an e-beam, consisting of an ensemble of electrons, contains therefore, in principle, the information on energy and parallel velocity spreads. It has to be noticed, that depending on the angle θ one can either be sensitive to the e-beam energy ($\theta = \pi/2$) or to the parallel velocity ($\theta = 0$) spreads. In order to be outside of the spectral region of the relativistic cyclotron frequency, where parasitic oscillations have been observed ($f \simeq 100\,\mathrm{GHz}$) [2], all ECE-measurements have been performed at an angle $\theta = 15°$. The observed frequency upshift is about 40 GHz for our beam parameters.

An important difference between the ECE diagnostic and the commonly used retarding potential diagnostic is the fact that ECE can be performed at full beam parameters, whereas the retarding potential is always applied at reduced beam parameters which implies that perturbative effects on the e-beam properties (parasitic oscillations in the beam tunnel) cannot be observed.

Analysis of experimental results

The experimental set-up is described in detail in reference [1]. A typical measured ECE-spectrum is shown in figure 1 (dashed line). Since beam trajectory codes, e.g. EGUN or DAPHNE [4, 5], do not take into account any AC effects, the only source of energy spread in these codes is due to DC self-fields (potential depression), and the calculated energy spread is consistent with the assumption of a monoenergetic beam. In this case the relation between perpendicular and parallel velocity spreads is given by: $\delta\beta_\perp = \Delta\beta_\perp / <\beta_\perp> = \alpha^2 \Delta\beta_\parallel / <\beta_\parallel>$. When the cathode surface roughness is neglected, the velocity distribution function is mainly determined by the gun geometry and the distribution has in this case more a top-hat like rather than a Gaussian shape. Nevertheless, for the calculated spectrum in figure 1, the assumption of a Gaussian parallel velocity distribution has been made.

For the observation angle $\theta = 15°$ considered in this experiment the ECE-spectrum is mainly determined by the parallel velocity spread and not by the energy spread as shown in figure 2 since it is very unlikely that parasitic oscillations generate energy spreads larger than $\delta\gamma = \Delta\gamma/\gamma > 1\,\%$. However, the efficiency of a quasi-optical gyrotron (QOG) [3] changes significantly for an energy spread of the order of $\delta\gamma \simeq 1\,\%$ whereas the dependence on the parallel velocity spread, $\delta\beta_\parallel$, is much less pronounced (Fig. 3). Consequently, an additional ECE-measurement at a larger angle $\theta \simeq 60°$ is required (see figure 2) in order to simultaneously obtain energy and parallel velocity spreads.

One can see that the measured spectrum has a Gaussian like distribution and its width is 2–3 times larger than the calculated one assuming a Gaussian distribution in the parallel velocity with the mean and its spread given by the code DAPHNE with no surface roughness taken into account. A good agreement is, however, found between measured and calculated mean quantities. Finally, the results presented might be a consequence of cathode surface roughness ($\simeq 5\,\mu\mathrm{m}$) but no information can be extracted yet about the energy spread of the beam.

The space charge neutralization effect is shown in figure 4 where the mean frequency value of the emitted spectrum is plotted as a function of time for a beam current of 4.5 A. For reference a typical trace of the modulation voltage is shown. All other system parameters are as stable as the one shown. The measured increase of the mean frequency is due to an increase of the mean parallel velocity caused by a partial space charge neutralization of

PARASITIC MODE EXCITATION IN GYROTRON BEAM TUNNELS

M. Pedrozzi, S. Alberti, M. Q. Tran

Centre de Recherche en Physique des Plasmas
Association Euratom Confédération Suisse
Ecole Polytechnique Fédérale de Lausanne
21 Av. des Bains, CH-1007 Lausanne

Abstract

Experimental measurements of parasitic oscillations exited in Quasi-Optical Gyrotron (QOG) beam tunnels will be presented for different beam tunnel configurations. The observed starting current of such modes can be very low (100 mA), and the frequency is in general less than the maximum relativistic cyclotron frequency encountered in the beam tunnel. Estimations of the emitted RF power in parasitic modes is as high as 2kW for a beam power of 70 kW (V_k=70 kV, I_b=1A, $\alpha=v_\perp/v_\parallel$=1.12).

Introduction

Energy and velocity spreads induced by parasitic oscillations in the drift tube can be one of the reasons of the low efficiency observed in the CRPP QOG [1]. Figure 1 illustrates the relative power importance of Fabry-Perot TEM_{00q} modes and parasitic oscillation. Circles are associated with parasitic oscillations, squares with a Fabry -Perot TEM_{00q} mode. Filled points represent frequency, empty points power. It has to be noticed that parasitic oscillations persist for beam current higher than the minimum starting current of the QOG resonator modes (~1.3 A).

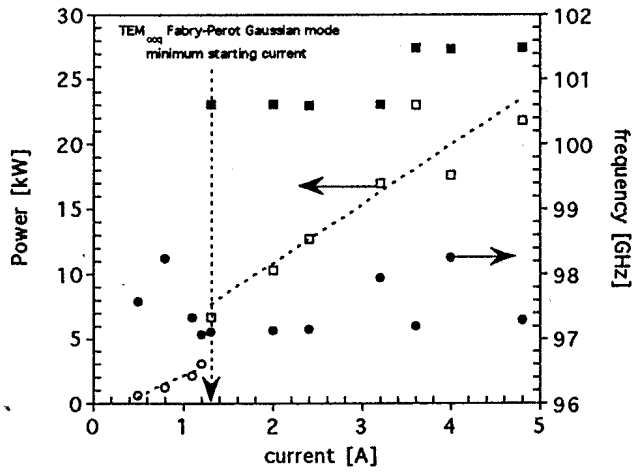

Figure 1. Power versus beam current in the 100 GHz QOG normal operation

Similar results are reported by Antakov et al. for a 35GHz cylindrical cavity gyrotron [2]. The importance of the beam tunnel damping structure is well assessed [3], unfortunately at high frequency this structure is highly overmoded and the damping rate optimisation becomes complicate. The QOG configuration is probably more sensitive to this problem due to the particular magnetic field structure (Fig.2), which presents a relatively long portion with small gradients in the beam tunnel region.

Experimental set up

The parasitic oscillations investigation is made on the 100 GHz QOG test stand[1]. Contrary to the case shown in Fig.1, oscillation in TEM Gaussian mode of the Fabry-Perot resonator was suppressed by inserting in front of one of the mirrors a strongly absorbing material (Macor). Different structures were tested. Two absorbers were used in this experiment, the Ceraloy 60%AlN-40%SiC and the Ceraloy 95%MgO-5%SiC. The drift tube structure is composed by alternate rings of copper (typical radius 5 mm) and absorber.

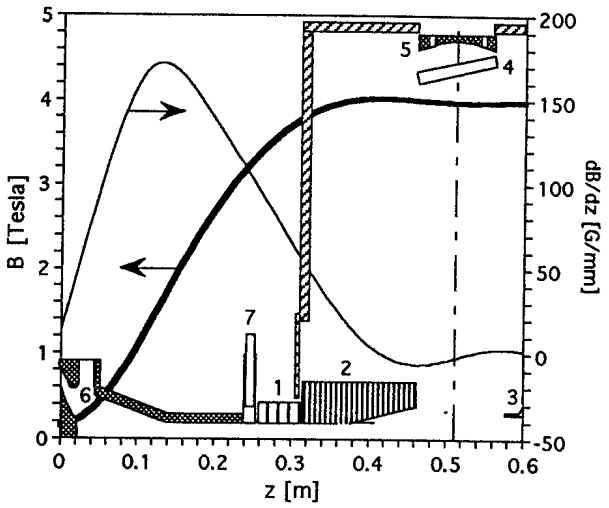

Figure 2. - The beam tunnel region with the tapered beam tunnel. (1. MgO-SiC 5%, 2. AlN-SiC 60%, 3. smooth wave guide r=8 mm, 4 Macor plate, 5. cavity mirror, 6 triode gun, 7. Gun vacuum valve)

A simpler configuration, consisting of a constant radius smooth beam tunnel, was also studied, and allowed a simplified theoretical modelling of the problem.

Experimental measurements

Magnetic field variation near the experimental starting current region.

The beam voltage was fixed at 64.5 kV, the velocity ratio α near the magnetic field maximum was 0.8-0.9 and the beam current was I_b≈200 mA. In Figure 3 the empty points correspond to a smooth beam tunnel and the filled points to a tapered beam tunnel. The horizontal lines

the beam. This result is consistent with an independent measurement made with a capacitive probe.

Conclusion

ECE emission has proven to be a powerful diagnostic for gyrotron electron-beams. Within the assumption of a monoenergetic beam the presented results agree with previous observations [6] concerning the perpendicular velocity spread measured with a retarding potential technique. Due to the presence of parasitic oscillations in the beam tunnel we believe that the monoenergetic assumption is invalid for our experiment. In order to measure the energy spread a measurement of the ECE emission at two different viewing angles ($\theta = 15°$ and $\theta = 60°$) will be performed.

The work was supported by the Fonds National de la Recherche Scientifique and by the Office Fédéral de l'Education et de la Science.

References

[1] G. Soumagne et al., 19^{th} *Int. Conf. on Infrared and Millimeter Waves* , Sendai 1994, JSAP Catalog No: AP 941228, 468–469, 1994.

[2] M. Pedrozzi, S. Alberti, M.Q. Tran, *this conference proceedings.*

[3] S. Alberti et al., *Phys. Fluids* **B2**, 1654–1661 (1990).

[4] W.B. Hermannsfeldt, *Tech. Report SLAC* **166**, 1973.

[5] R. Gruber et al., 16^{th} *Int. Conf. on Infrared and Millimeter Waves* , Lausanne 1991, SPIE 1576, 450–451 (1991).

[6] B. Piosczyk, 18^{th} *Int. Conf. on Infrared and Millimeter Waves* , Colchester 1993, SPIE 2104, 450–451 (1993).

Figures

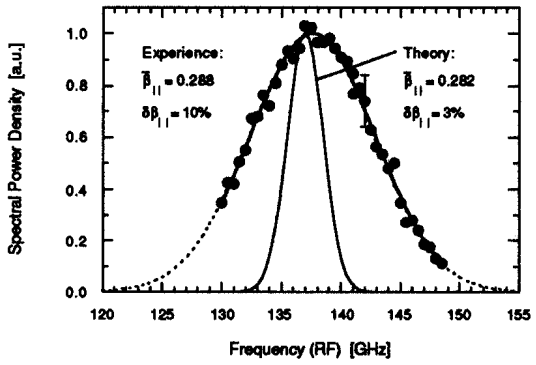

Figure 1: Experimental and calculated spectrum. Electron beam parameters: cathode voltage: −62 kV; modulation voltage: 28.8 kV, beam current: 1.5 A.

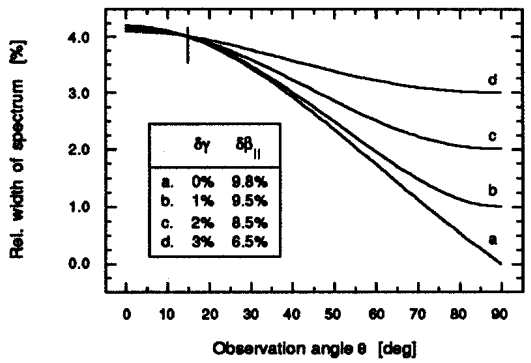

Figure 2: Relative spectral width of the ECE-spectrum as a function of the observation angle, θ, for different relative widths of the distribution functions of the parallel velocity, $\delta\beta_{\parallel}$, and the relativistic factor, $\delta\gamma$; the width of the spectrum at 15° has been fixed to 4 %; $<\beta_{\parallel}>= 0.3$.

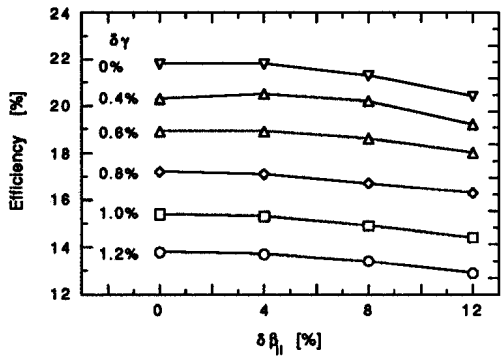

Figure 3: Calculated efficiency of the QOG as a function of the relative width of the distribution function of the parallel velocity, $\delta\beta_{\parallel}$, and the relativistic factor, $\delta\gamma$.

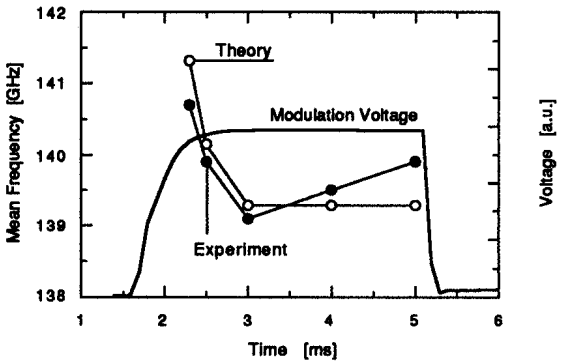

Figure 4: Temporal evolution of the mean frequency of the ECE-spectrum and a typical trace of the modulation voltage; cathode voltage: −62 kV; modulation voltage: 27.5 kV, beam current: 4.5 A.

represent the cut-off frequency of a cylindrical smooth wave guide of 5mm radius.

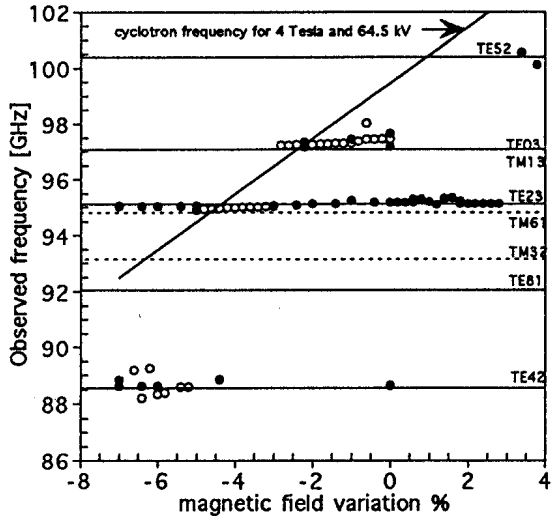

figure 3. Parasitic oscillation frequency versus magnetic field variation., ∂B=0% correspond sto Fig. 1.

The magnetic field scan of figure 3, performed at low current, shows that two different beam tunnels can support parasitic oscillations approximately at the same frequencies. In the smooth beam tunnel case, the TE_{23} transverse mode is excited over a magnetic field variation of $\Delta B/B=10\%$. It is possible to understand this phenomena if we imagine that the axial position where the mode starts to grow changes with the magnetic field variation. The beam tunnel length appears consequently to be an important parameter in the parasitic oscillation excitation.

Alpha variation, tapered beam tunnel case.

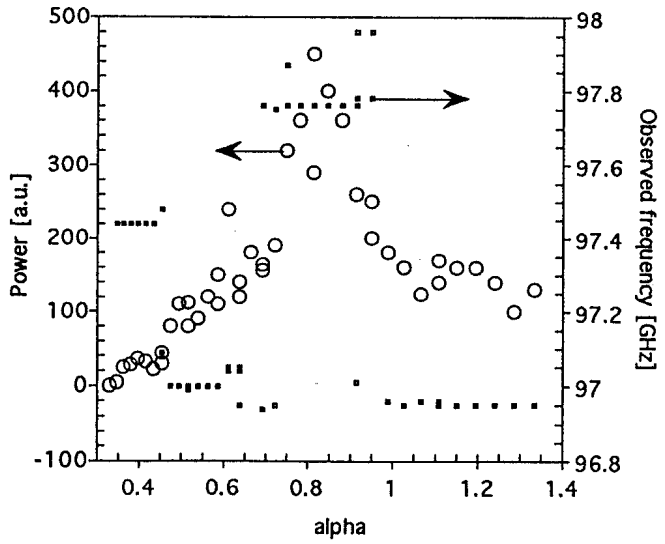

figure 4. Parasitic oscillation frequency and power versus velocity ratio. Vk=64.5 kV, Ib=2.5 A .

In Figure 4 an α scan shows that parasitic oscillations are excited in a large beam parameters domain. The filled squares correspond to the frequency and power is represented by empty circles. Similar results were observed for 45 and 55 kV beam voltages. As can be observed from Fig. 3 and 4, a discrete mode structure, (Δf 2-4 GHz) corresponding to different transverse mode is observed as well as a finer structure (Δf 100-800 MHz) probably due to excitation of different longitudinal modes for the same transverse mode. Starting current calculations of the cyclotron maser instability in a smooth cylindrical structure with varying magnetic field, indicate that backward wave oscillation are probably responsible for the excitation of parasitic oscillation. This effect is only possible if we consider higher order longitudinal TE_{mnq} modes (q>1), which can become unstable for negative detunings (backward wave) and are also very insensitive to magnetic field gradients [2]. Cold tests measurements show quality factors, Q, of the order of 5000-10000 for the smooth beam tunnel case. Using these quality factors measurements for the starting current calculation, good agreement is found between theory and experiment. Within linear theory, the calculated energy spread ($\Delta\gamma/\gamma=0.8\%$) is sufficient to importantly reduce the QOG efficiency [4].

Conclusions

In the quasi optical gyrotron parasitic oscillations are strongly excited in a large beam parameter domain and discrete mode structure was observed. The measured frequency is usually less than the relativistic cyclotron frequency of the maximum magnetic field, which suggest that backward wave oscillations are excited. Large quality factors Q are probably responsible for the observed low starting current. To confirm the correlation between the observed QOG low efficiency and the parasitic oscillation excitation, the beam parameters (parallel velocity $\partial\beta_{//}$ and energy $\partial\gamma$ spread) will be measured in the cavity gap using a diagnostic based on electron cyclotron emission [4].

Acknowledgements

This work was partially supported by the Swiss National Science Foundation.

References

[1] S. Alberti, et al, Phys. Fluids B 2 (7), 1990, pp.1654-1661
[2] I. Antakov, et al, IEEE Trans. on Plasma Science, vol.22 NO5.,1994, pp.878-882.
[3]W. Lawson, et al, IEEE trans. on Plasma Science, vol.20, NO3, 1992, pp.216-223.
[4] G. Soumagne, et al, in the IR & MM Waves present Proceedings, 1995.

STARTUP METHODS FOR SINGLE-MODE GYROTRON OPERATION

D. R. Whaley, M. Q. Tran, S. Alberti, T. M. Tran
Centre de Recherches en Physique des Plasmas, Association Euratom-Confédération Suisse,
Ecole Polytechnique Fédérale de Lausanne, 21 Av. des Bains, CH-1007 Lausanne, Switzerland

T. M. Antonsen, Jr.
Institute for Plasma Research and Departments of Electrical Engineering and Physics,
U. of Maryland, College Park, MD 20742

A. Dubrovin, C. Tran
Thomson Tubes Electroniques, 2 Rue Latécoère, 78140 Vélizy-Villacoublay, France

Abstract

Experimental results of startup studies on a 118GHz $TE_{22,6}$ gyrotron are presented and compared with theory. The startup paths through the energy-velocity-pitch-angle plane are determined by the time evolution of the beam parameters during the startup phase. These startup paths are modified by changing the anode and cathode voltage rise from zero to their nominal values and are seen to determine the cavity oscillating mode. Experimental results show specifically that competition between the $TE_{22,6}$ and $TE_{-19,7}$ mode can be completely eliminated by use of the proper startup method in a case where a typical triode startup results in oscillation in the competing $TE_{-19,7}$ mode. These new results are shown to be in excellent agreement with theory whose approach is general and therefore applicable to gyrotrons operating in any arbitrary cavity mode.

Introduction

In the design and operation of high-order mode gyrotrons mode competition must be considered to assure oscillation in the proper mode. Oscillation in a competing mode can result in a decrease of interaction efficiency, degraded performance of the quasi-optical coupling system, change in oscillation frequency, increase in window reflection, decrease of coupling between window RF power and the RF transport system. The dense mode spectrum of high-order modes requires consideration of the temporal evolution of the beam parameters during the startup phase. Here we apply the theoretical approach presented in [1] to experimental startup studies of a 118GHz 0.5MW gyrotron tube [2].

Startup Scenarios

In this study competition between the desired $TE_{22,6}$ operating mode and the competing $TE_{-19,7}$ mode is considered. Excitation regions of both modes are computed in the α-E plane where α is the velocity pitch ratio, $v_\perp/v_{//}$, and E is the beam energy. The startup path through the α-E plane depends on the startup scenario i.e. the method in which the anode and cathode voltages of the gyrotron are raised from zero to their nominal values. The choice of startup scenario determines the evolution of the beam energy, velocity pitch angle and beam current during the time-changing portion of the electron beam pulse. Depending on the path taken, one of the competing modes will be excited first and will grow to large amplitude. This mode can suppress all other competing modes even when the final beam parameters are such that another startup path would have resulted in excitation and oscillation of another mode.

A non-linear time-dependent code [3] has been used to validate the theoretical curves of Figs. 1-3. A full description of the method is found in [1] and [2].

Experimental Results

Experimental verification of the startup theory presented in [1] has been performed on a 118GHz gyrotron with a triode electron gun [4]. The scenario used for gyrotron startup is seen to be of great importance in determining the gyrotron oscillating mode. An optimum 'timed' scenario is found in which the anode and cathode voltages are first brought to intermediate values, V_{A1} and V_{K1}, and then increased simultaneously to the nominal values V_{A2} and V_{K2} as shown in Fig. 1(a). With this timed method, the startup path in the α-E plane is different than

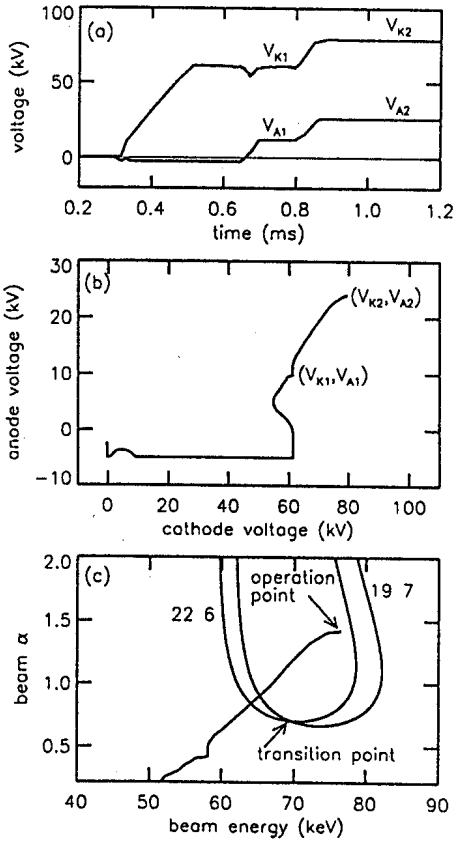

Figure 1. (a) experimental anode and cathode voltage forms for timed startup scenario. (b) voltages of (a) plotted in x-y (c) respective experimental startup path in the α-E plane. Excitation regions of the $TE_{22,6}$ and $TE_{-19,7}$ modes are also shown.

that of a typical triode scenario (with V_A increasing only after full V_K is established) where a vertical path is traced in the α-E plane Both triode and timed startups are possible in the experiment. Figures 1 show an experimental time trace of a timed startup. Fig. 1(a) is the oscilloscope trace of the voltages plotted in x-t, Fig. 1(b) is the same trace plotted in x-y, and Fig. 1(c) shows the actual startup paths converted to the α-E plane.

Frequency measurements show the two most dominant modes of the gyrotron to be the desired $TE_{22,6}$ mode and the competing $TE_{-19,7}$ mode. The excitation regions for these two modes are computed and also shown in Fig. 1(c). One can see that the startup path of the electron beam will move into the excitation region of one of the two modes first, exciting that mode before any other. The point at which the transition between the $TE_{22,6}$ mode and the $TE_{-19,7}$ mode occurs is labeled 'transition point'. Many startup paths, similar to that of Fig. 1(c), for a series of V_{A1}, V_{K1} combinations were performed for equal final nominal anode and cathode voltages. This merely affects the startup path approaching the same operation point. It is seen experimentally that depending on the startup path chosen, the tube oscillates in either in the $TE_{22,6}$ mode at a full power of P_H~0.5MW at f=118.0GHz or in the $TE_{-19,7}$ mode at a reduced power of P_H~0.1MW at f=117.5GHz. Once either mode is established it remains the oscillating mode for the remainder of the microwave pulse.

An enlargement of the region around the transition point of Fig. 1(c) is shown in Fig. 2 as well as the series of experimentally measured startup paths in a startup series with varying V_{A1} and V_{K1}. The values of V_{A1} and V_{K1} are chosen such that the paths lie on either side of the transition point. In the figure the paths which result in excitation of the $TE_{22,6}$ mode are shown as solid lines and the paths which result in excitation in the $TE_{-19,7}$ mode are shown as dotted lines. It is readily seen that all combinations of V_{A1}, V_{K1} passing first into the $TE_{22,6}$ excitation region result in oscillation in the proper $TE_{22,6}$ mode and combinations of V_{A1}, V_{K1} passing first into the $TE_{-19,7}$ excitation region result in oscillation of the $TE_{-19,7}$ mode. In general a high V_{A1} and low V_{K1} eliminates the problem of competition with the $TE_{-19,7}$ mode. It should be noted that a typical triode startup also results in low power oscillation of the $TE_{-19,7}$ mode.

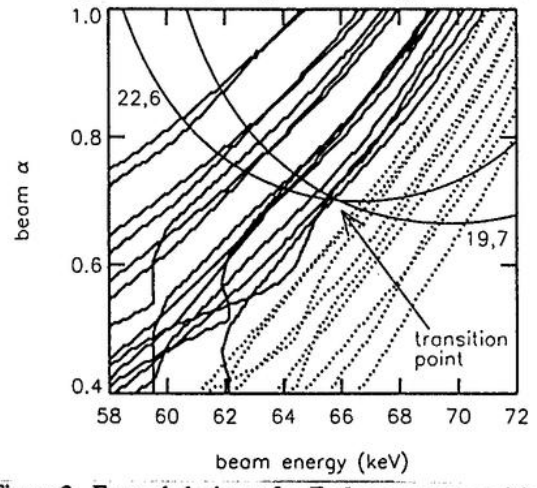

Figure 2. Expanded view of α-E plane near transition point. Each line represents the experimental startup path followed by a separate shot. Solid paths represent shots that startup and oscillate in the $TE_{22,6}$ mode (0.5MW) and dotted paths represent shots that startup and oscillate in the $TE_{-19,7}$ mode (0.1MW). Theoretical excitation regions for both modes are also shown.

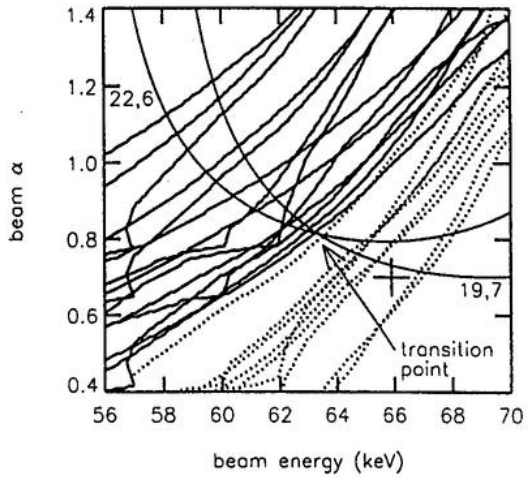

Figure 3. As with Fig. 2 for second startup series. The beam compression has been changed to decrease the beam radius in the cavity by 0.02a. The transition point of the first startup series shown in Fig. 2 has been marked with a '+'.

Another experimental startup series was taken with the transition point of Fig. 2 moved in the α-E plane. This was accomplished by slightly increasing the beam compression. Startup in the $TE_{22,6}$ or the $TE_{-19,7}$ mode was again determined as a function of the startup path. The result is shown in Fig. 3. As in Fig. 2, Fig. 3 shows that only startup paths entering the excitation region of the $TE_{22,6}$ mode result in final oscillation of the $TE_{22,6}$ mode. Also, with the transition point changed in Fig. 3, combinations of V_{A1}, V_{K1} that, in Fig. 2 led to $TE_{22,6}$ oscillation, now result in oscillation of the $TE_{-19,7}$ mode as expected.

Conclusions

The temporal evolution of the electron beam during gyrotron startup is seen to be important to mode selection in high-order mode gyrotrons. In the experiments presented here, high power oscillation in the desired $TE_{22,6}$ mode is shown to occur only with the correct startup scenario where a typical triode startup results in low power oscillation in a competing mode.

The contribution and assistance during these tests of P. Garin, E. Giguet, J.-M. Krieg, and H.-G. Mathews of Thomson Tubes Electroniques (TTE), M. Pain of the CEA and M. Thumm of the FZK were greatly appreciated. The 118 GHz gyrotron was constructed in the framework of a joint development between the Associations Euratom - CEA Cadarache, Euratom - Swiss Confederation and TTE. This work was partially supported by the Swiss National Science Foundation.

[1] D. R. Whaley et al., IEEE Trans. Plasma Sci. **22**, 850 (1994).
[2] D. R. Whaley et al., Phys. Rev. Lett. **75**, 1304 (1995).
[3] S. Y. Cai et al., Int. J. Electron. **72** 759, (1992).
[4] M. Pain et al., in Proceedings of the 18th Symposium on Fusion Technology, Karlsruhe, 1994, pp.489-492 and E. Giguet at this conference..

Cold Tests and High Power Measurements on an Advanced Quasi-Optical Mode Converter for a 118 GHz Gyrotron

O. Braz, M. Losert, A. Möbius, M. Thumm

Forschungszentrum Karlsruhe, Association EURATOM-FZK,
Institut für Technische Physik, P. O. Box 3640, D-76021 Karlsruhe, Germany
and Universität Karlsruhe, Institut für Höchstfrequenztechnik und Elektronik

R. Coudroy, E. Giguet, C. Tran

Thomson Tubes Electroniques
2, rue Latécoère, 78141 Vélizy Villacoublay, France

M. Q. Tran, D. R. Whaley

Centre de Recherches en Physique des Plasmas, Association Euratom Confédération Suisse,
Ecole Polytechnique Fédérale de Lausanne
21 Av. des Bains, CH-1007 Lausanne, Switzerland

Abstract

This paper reports on cold test and high power measurements of the improved, dimple type quasi-optical mode converter for the 118 GHz, 0.5 MW, 210 s $TE_{22,6}$ gyrotron oscillator collaboratively developed by CEA Cadarache, CRPP Lausanne, FZK Karlsruhe and Thomson Tubes Electroniques Vélizy. For the low power measurements the required rotating $TE_{22,6}$ mode was generated in a coaxial cavity using quasi-optical techniques. The high power measurements were performed on the gyrotron output beam using an infrared camera. The evaluated mode purity of the linearly polarized fundamental Gaussian output mode is (96 ± 1)% in agreement with calculations.

1. Introduction

To separate the RF-Power from the electron beam and to generate a linearly polarized TEM_{00} output mode, an improved quasi-optical mode converter is incorporated into the vacuum system of the Thomson quasi-cw 0.5 MW 118 GHz $TE_{22,6}$ gyrotron. The converter consists of a rippled-wall waveguide launcher followed by a phase correcting mirror of quasi-parabolic shape and two toroidal reflectors, where the astigmatism is removed and the output beam transverse dimension are matched to the window size (beam waist $w_0 \approx$ 23 mm). The purpose of the irregular feed waveguide section is to convert the incident rotating $TE_{22,6}$ mode into an appropriate mode mixture generating a Gaussian distribution [1]. To keep the deformed feed waveguide (helical $\Delta m = 1$ and 3 perturbations) short, it is necessary to have an antenna radius of 20 mm corresponding to a Brillouin angle of about 67.3°. Coupled mode theory is used in the design and analysis of the launcher, and the reflectors are designed with Gaussian optics and vector diffraction theory. The quasi-parabolic mirror is tilted to correct the offset of the center reflected ray. To verify the proper behavior of the quasi-optical mode converter and to determine the parameters of the gyrotron output beam high power measurements using an infrared camera, as suggested in [2], have been performed. Alternatively an identical mode converter system has been built for low power tests. To compare the results with theory a computer code using Huygens' principle was used. The beam parameters are evaluated from the measured and calculated field patterns maximizing the following efficiency coefficient:

$$\eta_0 = \frac{\left(\iint \sqrt{M(x,y)} \cdot \sqrt{G_0(x,y)}\, dx\, dy\right)^2}{\iint M(x,y)\, dx\, dy}$$

Where $G_0(x,y)$ is the normalized fundamental Gaussian function and $M(x,y)$ represents the measured or calculated power distribution.

2. Calculations

Starting with the calculated field pattern at the location of the first mirror, which is in good agreement with the cold tests, the transformation of the beam through the mirror system has been analyzed by a computer code applying Huygens' principle. The theoretical overall conversion efficiency is 93%. Fig. 1 shows a power contour plot calculated at a distance D = 1420 mm in front of the gyrotron output window.

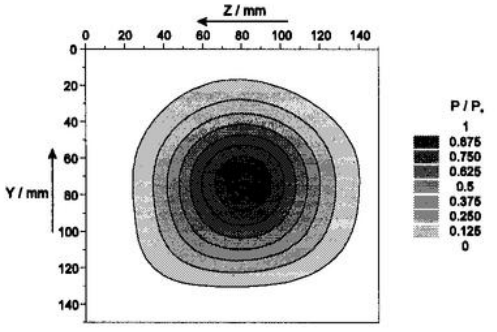

Fig. 1: Power pattern calculated at D = 1420 mm

3. Cold Test Measurements

Fig. 2 gives an overview of the low power measurement setup.

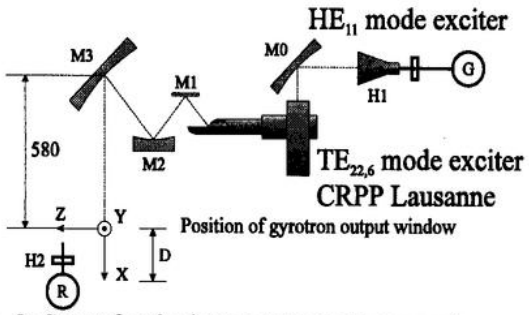

Fig. 2: Setup for the low power measurements.

For the millimeter wave detection a scalar network analyzer [3] has been used. The required rotating $TE_{22,6}$ mode was produced in a coaxial cavity using quasi-optical techniques [4]. Fig. 3 shows a power contour plot measured at a distance D of 1450 mm in front of the gyrotron output window.

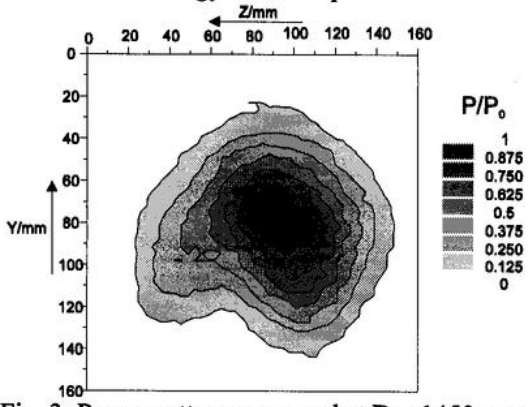

Fig. 3: Power pattern measured at D = 1450 mm

4. High Power Measurements

To measure the structure of the gyrotron output beam a specific dielectric target plate was placed at several cross-sections of the beam. The thermal image appearing by passing of microwave radiation through the target material was recorded by an infrared camera. Fig. 4 shows the temperature distribution of the beam at a distance D of 2150.8 mm in front of the gyrotron output window.

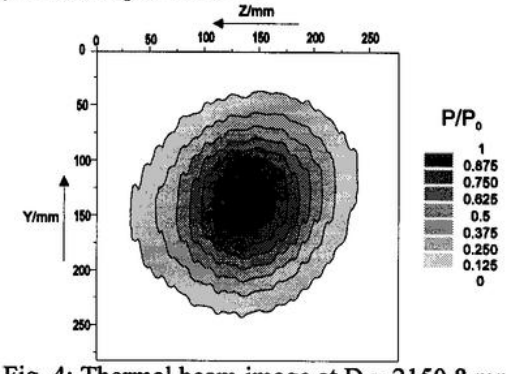

Fig. 4: Thermal beam image at D = 2150.8 mm

5. Discussion of Results

Figs. 5 and 6 show the determined beam parameters versus the distance from the gyrotron output window. The beam waist parameters are found by fitting the theoretical 1/e field radius dependency to the data. The agreement between the parameters determined by low power tests and those given by calculations is rather good. However the beam waist produced in the low power setup is about 1-3 mm larger and shows a more elliptical shape. This may be due to a small parasitic $\Delta m = 1$ mode content of the $TE_{22,6}$ mode exciter. Compared to the cold measurements and calculations the position of the beam waist in the high power measurements is too far inside the tube. Whether this is a problem of thermal dispersion of the target or not is at the moment under investigation. Nevertheless the experimentally determined purity of the linearly polarized TEM_{00} output mode is (96 ± 1)% in agreement with theory. The orthogonal polarization was measured to be lower than -16dB.

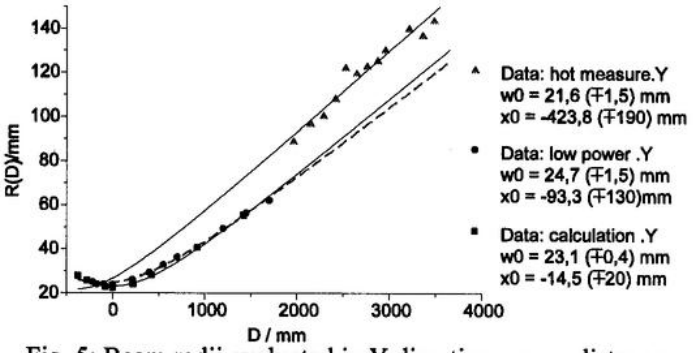

Fig. 5: Beam radii evaluated in Y direction versus distance from the gyrotron output window

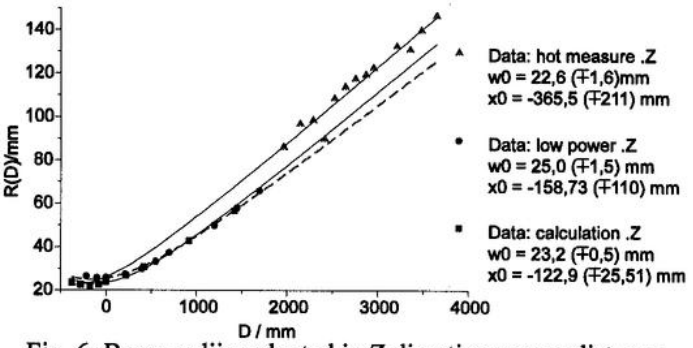

Fig. 6: Beam radii evaluated in Z direction versus distance from the gyrotron output window

Cold test measurements are very useful to detect large design errors or to use in the alignment of the converter assembly. In order to achieve results, useful for a final design, one must provide a waveguide mode of a very high purity.

References

[1] G.G. Denisov, et al., Int. J. Electronics, **72**, 1079-91, 1992.

[2] S. O. Kuznezov,V. I. Malygin, Int. J. Infrared and Millimeter Waves, **12**, 1241-1252, 1991.

[3] T. Geist, G. Hochschild, W. Wiesbeck, Proc. 18th European Microwave Conf., Stockholm, pp. 339-343, 1988.

[4] N. L. Alexandrov, G. G. Denisov, D. R. Whaley, M. Q. Tran, Low power excitation of gyrotron-type modes in cylindrical waveguide using quasi-optical techniques,accepted for publication in Int. J. Electronics, March 1995.

Operation of a 118 GHz - 0.5 MW Gyrotron with Cryogenic Window: Design and Long Pulse Experiments

E. GIGUET, A. DUBROVIN, J.M. KRIEG, Ph. THOUVENIN, C. TRAN
Thomson Tubes Electroniques, 2 rue Latécoère, 78141 Vélizy-Villacoublay, France

P. GARIN, M. PAIN
Association Euratom-CEA, Département de Recherches sur la Fusion Contrôlée
13108 Saint Paul lez Durance, France

S. ALBERTI, M.Q. TRAN, D.R. WHALEY
Centre de Recherches en Physique des Plasmas, Association Euratom-Confédération Suisse
Ecole Polytechnique Fédérale de Lausanne, 21 Av. des Bains, CH-1007 Lausanne, Switzerland

E. BORIE, O. BRAZ *, A. MÖBIUS, B. PIOSCZYK, M. THUMM *, A. WIEN *
Forschungszentrum Karlsruhe, Association Euratom-FZK
Institut für Technische Physik, P.O. Box 3640, D-76021 Karlsruhe, Germany
* and Universität Karlsruhe, Institut für Höchstfrequenztechnik und Elektronik

Abstract

A 210 s, 0.5 MW, 118 GHz gyrotron with a cryogenic window has been designed, constructed and tested as a joint collaboration between CEA-Cadarache, CRPP-Lausanne, FZK-Karlsruhe and TTE-Vélizy for ECRH experiments on Tore Supra and TCV. The gyrotron operates in a $TE_{22,6}$ cavity mode and provides a TEM_{00} mode, converted into a HE_{11} mode in an external Optics Unit. It is composed of a triode-type electron gun, an improved beam tunnel, a high-mode-purity low-ohmic-loss cavity with an optimized non linear taper, a highly efficient internal quasi-optical mode converter, a large collector with a beam sweeping magnet, and a horizontal RF output through a liquid nitrogen edge-cooled single-disk sapphire window[1]. Output powers of 0.7 MW- 0.1 s and 0.5 MW - 2 s have been achieved with the desired frequency, efficiency and mode pattern.

Frequency	118 GHz
Output power	0.5 MW
Pulse duration	210 s
Duty cycle	33 %
Output mode	HE_{11}
Output mode purity	> 95 %
Efficiency (output power in HE_{11} / beam power)	> 30 %
Cathode voltage	< 85 kV
Beam current	< 22 A
Anode voltage	< 30 kV

Table 1: 118 GHz gyrotron main characteristics.

Design

The main theoretical parameters of the 118 GHz gyrotron are given in Table 1, and a schematic diagram is shown in Figure 1. The triode-type electron gun has been designed to produce a beam with a velocity ratio of α=1.5, and the electrodes of the MIG have been shaped to provide a low dispersion of $\Delta\alpha/\alpha$=2% required for high efficiency interaction and low probability of mirroring. The cavity α of the beam as a function of cathode emission location is essentially constant. The design also allows for a low electric field (61 kV/cm) on the surface of the emitter and low radial spread (2 %) of the beam in the cavity.

The cavity is designed to operate in the $TE_{22,6}$ mode with parameters chosen to allow for low peak wall losses (<1kW/cm^2 for cold ideal copper) and to minimize cavity sensitivity to power reflection and possible manufacturing errors. The relatively short cavity and high Q are achieved by use of a small iris at the cavity output. Mode conversion is reduced by use of angle roundings and of a non linear output uptaper. The resulting mode purity is calculated to be 99.8 % instead of 94.5 % with no roundings and a linear taper.

The RF beam is separated from the electron beam through an improved quasi-optical mode converter consisting of a rippled-wall waveguide launcher followed by a phase correcting mirror of quasi parabolic shape and two toroidal focusing mirrors which match the beam to the window size (waist of 23 mm). The high theoretical conversion efficiency has been confirmed by cold tests showing a mode purity of the linearly polarized TEM_{00} of 96 ± 1 % [3].

Because of the output Gaussian profile, a conventional window could not be used for CW operation (typical limitation between 0.3 and 0.4 MW). Among the existing solutions, we have chosen a cryogenic window consisting of a single sapphire disk cooled on its edge by liquid nitrogen. The disk thickness is 5 $\lambda/2$ to obtain low stress with atmospheric pressure, the outer diameter is 120 mm, much greater than the waveguide diameter (80 mm) in order to obtain a suitable exchange surface between sapphire and liquid nitrogen. Computations have shown that the thermal runaway occurs for power levels higher than 0.65 MW with a Gaussian profile[4].

Once extracted from the gyrotron, the power is converted

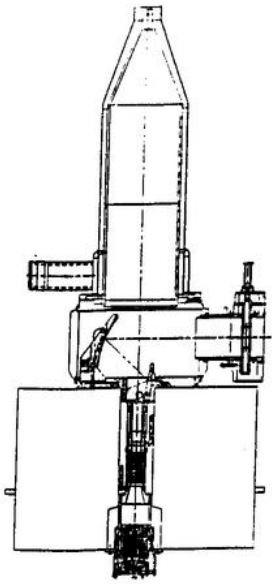

Figure 1: 118 GHz - 0.5 MW CW gyrotron with cryogenic window

into the desired HE_{11} mode, through an Optics Unit, consisting of two flat and moveable mirrors allowing for correction of possible minor errors in the RF profile and a focusing mirror which refocuses the beam prior to entering the corrugated waveguide.

Experimental Results

A short pulse tube has been constructed and tested to validate the design parameters. Power levels up to 625 kW with an efficiency around 30 % were obtained at the desired frequency, even if mode competition between the desired $TE_{22,6}$ mode and the $TE_{-19,7}$ mode was quite severe. This problem was corrected using the proper startup method [2]. Due to the poor cooling of this tube, the pulse length was limited to a few milliseconds.

A long pulse tube has now been tested. Mode competition is not a problem anymore and the output profile appears to be in good agreement with the predicted one (see Figure 2). The beam waists have been calculated to be 21.6 ± 1.5 mm in the horizontal direction and 22.6 ± 1.6 mm in the vertical direction.

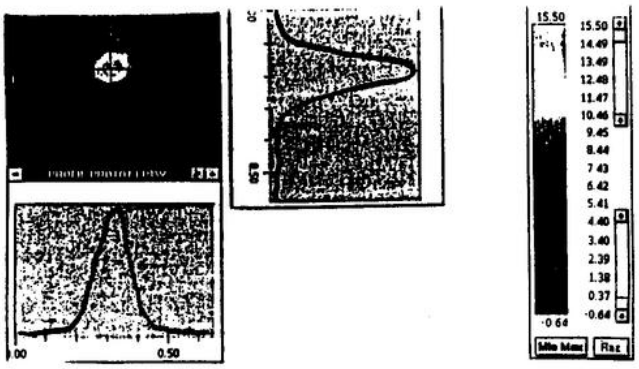

Figure 2: RF profile outside the tube - IR measurement

The tube behavior has been analyzed in short pulse operation. Figure 3 shows a plot of output power and efficiency versus beam current. The cathode and anode voltages as well as the magnetic field were adjusted to optimize the efficiency.

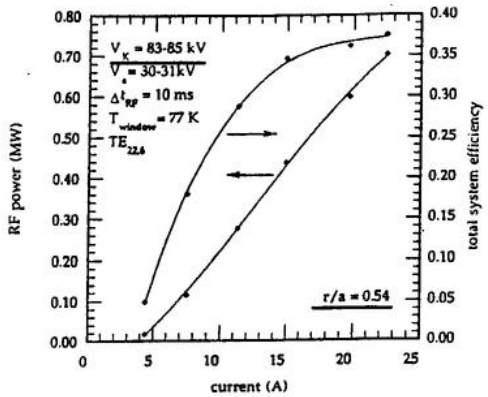

Figure 3: Output power and efficiency vs beam current

A power level of 0.7 MW has been reached with 37% total system efficiency. The main parameters for this point are: cathode voltage: 83.2 kV, beam current: 22.5 A, anode voltage: 30 kV, window cooled to 77 K.

The pulse length was then increased, with the power limited to 0.5 MW because of the window. No major difference was seen between long pulse and short pulse behaviors. Finally, a pulse length of 2 s (0.5 MW) has been reached with a cathode voltage of 80.5 kV, a beam current of 20 A and an anode voltage of 29 kV (31 % efficiency).

The cavity and launcher ohmic losses have been measured and appear not to exceed 50 kW.

Conclusion

The initial tests on the 118 GHz - 0.5 MW gyrotron have validated all the design parameters, especially the behavior of the cryogenic window. Further tests will be aimed at enlarging the pulse length up to 210 s.

The 118 GHz gyrotron development was constructed in the frame work of a joint development between the Associations EURATOM-CEA, EURATOM-Swiss Confederation and THOMSON TUBES ELECTRONIQUES.

The work performed at the CRPP is partially supported by the Swiss National Science Foundation.

References

[1] M. Pain et al., in Proceedings of the 18th Symposium on Fusion Technology, Karlsruhe, 1994, pp 489-492.

[2] D. R. Whaley et al., Phys. Rev. Lett., 75, 1304 (1995) and in these proceedings.

[3] O. Braz et al., "Cold Tests and High Power Measurements on an Advanced Quasi-Optical Mode Converter for a 118 GHz Gyrotron", in these proceedings.

[4] P. Garin et al. , "Cryogenically Cooled Window: a New Step toward Gyrotron CW Operation", in these proceedings.